HHS Public Access

Author manuscript

Curr Opin Biomed Eng. Author manuscript; available in PMC 2020 December 01.

Published in final edited form as:

Curr Opin Biomed Eng. 2019 December ; 12: 51–58. doi:10.1016/j.cobme.2019.09.007.

Optical Studies of Action Potential Dynamics with hVOS probes

Yihe Ma, **Peter O. Bayguinov**, **Meyer B. Jackson**

Department of Neuroscience, University of Wisconsin - Madison

Abstract

The detection of action potentials and the characterization of their waveform represent basic benchmarks for evaluating optical sensors of voltage. The effectiveness of a voltage sensor in reporting action potentials will determine its usefulness in voltage imaging experiments designed for the study of neural circuitry. The hybrid voltage sensor (hVOS) technique is based on a sensing mechanism with a rapid response to voltage changes. hVOS imaging is thus well suited for optical studies of action potentials. This technique detects action potentials in intact brain slices with an excellent signal-to-noise ratio. These optical action potentials recapitulate voltage recordings with high temporal fidelity. In different genetically-defined types of neurons targeted by cre-lox technology, hVOS recordings of action potentials recapitulate the expected differences in duration. Furthermore, by targeting an hVOS probe to axons, imaging experiments can follow action potential propagation and document dynamic changes in waveform resulting from use-dependent plasticity.

Introduction

Action potentials serve as an elementary all-or-none electrical signal used by the nervous system to perform a form of digitization of information. Action potentials come in elaborate trains in which the frequency of firing and precise temporal sequence is thought to serve important roles in neural network function [1,2]. Decoding these complex processes with voltage imaging techniques thus places a premium on the detection of action potentials. Furthermore, action potentials are not simple binary events, and their dynamic properties can vary widely. Action potential shapes differ between neuronal cell types and are often taken as a defining characteristic. For example, some inhibitory interneurons have narrow action potentials and are commonly referred to as ‘fast-spiking’ [3]. Action potential shapes can also vary at different stages of development [4]. Spikes generally rise more rapidly than they fall, and this asymmetry can vary between types of neurons [5]. Action potential shapes have an important impact on function. The amount of transmitter released from a synaptic terminal increases steeply with action potential duration [6–8]. Dynamic changes in action potential durations serve as a form of short term plasticity [9], and in nerve terminals are responsible for use dependent increases in secretion [10–12]. Furthermore, action potential

The authors declare no conflicts of interest

shape may differ between cellular compartments [12–15]. Action potentials can be observed in dendrites, somata, or axonal initial segments, and voltage imaging can identify the sub-millisecond timing differences between these compartments [14].

Voltage imaging provides a powerful approach to the study of these dynamic aspects of electrical signaling, and has the potential to investigate cellular compartments that are difficult or impossible to access with electrical recording techniques. However, because action potentials are brief events in which the voltage changes rapidly, their detection requires a voltage sensor with rapid response kinetics. Furthermore, going to the next level of characterizing spike shape makes even greater demands on a voltage sensor. Most synthetic voltage probes, organic molecules that act as voltage sensitive dyes, have rapid response times of 1.2 μs or less [16]. Optical recordings with such probes track action potentials with essentially perfect temporal fidelity [17,18]. Thus, synthetic dyes offer the greatest power for such studies, and have been used to make major contributions to dynamic electrical signaling in neurons [14,19–22].

Unfortunately, synthetic dyes are difficult to target to specific types of cells. Recent advances in harnessing genetic strategies to guide the expression of voltage sensors to neurons suggest that this approach has great potential for probing voltage dynamics in genetically-defined neurons [23–26]. Genetically-encoded voltage sensors can draw upon an extraordinary array of genetic targeting strategies [27]. However, genetically-encoded voltage sensors often depend on conformational transitions of a protein, and these processes generally occur over millisecond timescales. It has proven difficult to create genetically-encoded voltage sensors with response times fast enough for the facile study of action potentials [28,29]. The fast state transitions of opsins allows some opsin-based and hybrid FRET-opsin genetically-encoded voltage indicators to respond with sub-millisecond kinetics [30,31]. Opsin-based arch probes have been used to resolve presynaptic action potential waveforms in cultured hippocampal neurons [15,32], and study action potential repolarization at the *Drosophila* neuromuscular junction [33]. However, voltage indicators of this genre suffer from poor brightness and have yet to see use in the study of action potential waveforms in intact brain tissue.

This article discusses the requirements of probe response in detail and examines how a voltage sensor's time response influences the fidelity of action potential recordings. Hybrid voltage sensor (hVOS) imaging [34], offers a means of targeting a voltage sensor genetically [24], and hVOS probes are rapid enough to capture pertinent dynamic properties. These advantages are discussed and illustrated with examples. hVOS imaging tracks individual action potentials very well, follows their propagation, detects differences in spike characteristics between cell types, and reveals use-dependent changes in action potential properties.

Probe Kinetics and Action Potential Dynamics.

Action potentials are often characterized in terms of their width at half maximum (WHM), the interval from when the voltage is half-maximal on the way up to the time when the voltage is half-maximal on the way down. The WHM of action potentials varies widely in

mammalian central neurons, with values ranging from 0.18 to 4 msec [3]. Clearly voltage sensors must have msec response times to serve as effective spike detectors, and sub-msec response times to analyze their shapes.

Voltage sensors are characterized dynamically in terms of their exponential relaxation in response to a voltage step. To gain insight into how probe response time influences the observed properties of action potentials we start with an exponential relaxation function that describes the response kinetics of a generic probe.

$$F = F_f + (F_0 - F_f)e^{-t/\tau} \quad (1)$$

For a stepwise change in voltage from V_0 to V_f, the fluorescence, F, will relax exponentially from its initial value, F_0, at t=0, to its final value, F_f, at very large t. τ is the time constant, which depends on the dynamics of the particular probe. For a fixed voltage, fluorescence is proportional to voltage, $F_f = \alpha V_f$. When V varies with time then the dynamics of F can be understood by replacing F_f with αV, taking the time derivative of Eq. 1, and rearranging:

$$\frac{dF}{dt} = \frac{-(F - \alpha V(t))}{\tau} \quad (2)$$

The solution is

$$F(t) = \alpha e^{-t/\tau} \int_0^t V(s) e^{s/\tau} ds \quad (3)$$

where the initial value of F was arbitrarily set to 0. Since α is the proportionality constant it can be set to one in order to focus on the dynamic relation between F and V.

The Hodgkin-Huxley equations were used to generate an action potential triggered by a brief current pulse [35]. Taking this action potential as $V(t)$ and resetting the resting initial voltage to 0, this simulated action potential has an amplitude of 106 mV and a WHM of 1.48 msec (Fig. 1A). The fluorescence signals were then computed from the simulated Hodgkin-Huxley action potential using Eq. 3, with τ = 0.5, 1 and 5 msec (Fig. 1A). These plots illustrate that even with a one msec time constant, a voltage probe will reduce the amplitude and increase the WHM by ~60%. For a range of τ values, Fig. 1B plots the decrease in amplitude and Fig. 1C plots the increase in WHM. As noted above, action potential properties vary between cell types. The Hodgkin-Huxley equations represent the action potential of the squid giant axon, and this can be taken as a generic spike. The results in Fig. 1 thus provide a rough guide for how voltage sensors with different dynamic responses will impair detection and distort the shape of an action potential. However, it should be noted that briefer action potentials will be distorted more and longer action potentials will be distorted less.

Action Potential detection with hVOS

hVOS works through an optical (FRET) interaction between a membrane tethered fluorescent protein and a small non-fluorescent absorber, dipicrylamine (DPA) [34]. DPA

has the unusual combined properties of charge and hydrophobicity. It partitions into the lipid bilayer and its negative charge allows it to be pulled from one side of the membrane interior to the other by changes in voltage (Fig. 2A). The distance between the DPA and the chromophore within the fluorescent protein determines the strength of the FRET interaction between the two molecules. Thus, at negative membrane potentials the DPA is far from the fluorescent protein, FRET is weak, and fluorescence emission is high. Depolarization moves the DPA closer to the fluorescent protein and the stronger FRET interaction reduces emission. The original hVOS technique employed EGFP anchored to the membrane by an h-ras motif [34]. Testing a variety of probes and anchoring motifs led to a substantially better probe, composed of cerulean fluorescent protein anchored to the membrane by a truncated h-ras motif [36].

The response time of the hVOS technique depends on the time it takes DPA to traverse the membrane in response to voltage. This has been determined to be about 0.1 msec in guinea pig cardiac myocytes, *Xenopus* oocytes [37], squid axon [38], frog nerve [39], and HEK cells [40]. Thus, according to the above analysis (Fig. 1) hVOS probes should detect action potentials with high fidelity and produce minimal distortion of shape. In a study of probe performance in brain slices [41], hVOS probe was expressed in brain by two techniques, a non-specific technique, *in utero* electroporation, and a general neuron-specific technique, from the pan-neuronal thy1 promoter in transgenic mice [42]. An hVOS recording of an action potential from a patch clamped neuron illustrates that the fluorescence signal tracks the voltage change without a time lag (Fig. 2B). Note that the traces diverge at negative membrane potentials due to the nonlinearity of hVOS [34][36]. hVOS recordings from neurons in brain slices from cortex and hippocampus illustrate that action potentials produce fluorescence changes of ˜3% with a signal-to-noise ratio of 9–16 [41].

Action potential dynamics were also tested by targeting probe expression to specific types of cells. Using an hVOS Cre reporter mouse (Ai35-hVOS 1.5; available from JAX), the probe was targeted to various neuronal cell types by crossing with the appropriate Cre driver line [24]. Fig. 2C illustrates hVOS recordings of action potentials in calretinin interneurons (hVOS::Calb2), hilar mossy cells (hVOS::CalCrl), parvalbumin interneurons (hVOS::Parv), and inhibitory neurons defined by expression of the enzyme glutamic acid decarboxylase (hVOS::GAD2). WHM values for these and a few other cell types are presented in Fig. 2D. Some of these values differ significantly from one another and they follow a general trend of recapitulating known spike characteristics of different types of neurons [24].

The recordings in Fig. 2 were made in single trial recordings without averaging. This is important for characterizing spikes, because the timing of firing is intrinsically variable. Thus, aside from the issues discussed above regarding probe response time, averaging can also distort dynamics. The latency of a response can fluctuate by 1–2 msec from one trial to the next, and averaging will broaden events over this range to increase the WHM by a factor of two or more [24]. Thus, action potential shapes are much more difficult to study when averaging is necessary.

Action Potential Propagation

An hVOS probe has been developed that shows strong preferential targeting of axons [43]. This targeting was effected by incorporation of a sequence from the axonal protein GAP-43 to the N-terminus (the truncated h-ras motif is at the C-terminus) [36]. This hVOS probe variant was designated hVOS 2.0, and provides a unique opportunity to study action potential dynamics in axons with minimal interference from cell bodies and dendrites. A transgenic mouse generated with this axonal hVOS probe under the thy-1 promoter was found to express probe in the axons of granule cells of the dentate gyrus and mossy cells of the hilus (the axons of granule cells are generally referred to as 'mossy fibers'). Probe expression was high in the regions containing these axons, particularly in the stratum lucidum of the hippocampal CA3 region, which contains the mossy fiber axons of the granule cells (Fig. 3A), and in the inner molecular layer of the dentate gyrus, which contains the axons of hilar mossy cells (Fig. 3B). Traces from different sites illustrate how the action potential propagates away from the site of stimulation along the fiber track (Figs. 3A and 3B).

Traces such as those shown in Figs. 3A and 3B can be used to generate plots of time versus distance. The slopes then give the action potential conduction velocity (Figs. 3C and 3D). Conduction was slow in the finer axons of mossy cells (0.094 mm/ms in 2 μM DPA and 0.087 mm/ms in 4 μM DPA) and faster in the larger axons of granule cells (0.198 mm/sec in 2 μM DPA and 0.228 mm/ms in 4 μM DPA). The slightly lower velocities in higher DPA concentrations reflect the impact of DPA on membrane capacitance. The different velocities in different axons followed the well-established scaling with the square root of the diameter [43]. The WHM also differed between the two types of axons, and the WHM grew larger as the action potentials propagated in mossy cell axons but not in granule cell axons. Since these measurements were from populations of axons the increase in WHM suggests a dispersion of conduction velocities. This broadening of the population would have the potentially important consequence of reducing the synchrony of activation of postsynaptic targets [43].

Action Potential Broadening and Failure

Repetitive firing at high frequencies induced both broadening and failure of action potentials in both granule cell axons and mossy cell axons [43]. Action potential broadening had been demonstrated previously in granule cell axons because their boutons are large enough for patch clamp recording [12]. hVOS imaging in axons confirmed the prior work (Figs. 4A and 4C) and provided the first demonstration of this phenomenon in the much finer mossy cell axons (Figs. 4B and 4D). Action potential broadening became more pronounced as the stimulation frequency increased, but there was a significant difference in the amount of broadening between the two types of axons with trains of 10 Hz [43]. In granule cell axons this broadening had been shown to be associated with enhanced synaptic release [12] and it is likely that broadening of action potentials in the finer mossy cell axons has similar consequences.

Action potentials also fail with repetitive stimulation, and this serves as an important filtering mechanism in neural computation [44]. In both types of axons labeled by the axonal hVOS 2.0 probe, action potentials attenuated with repetitive stimulation. This can be seen when the traces are not normalized to their peaks (Figs. 4E and 4F). Comparisons of failure rates between sites near the site of stimulation and further away suggested that failure was due to an increase in firing threshold rather than conduction failures. Furthermore, the declines in amplitudes were similar between the axons of granule cells and mossy cells [43]. These experiments with an axonally-targeted genetically-encoded voltage sensor thus established fundamental aspects of action potential dynamics in two populations of axons in the hippocampus. One population, the granule cell axons, can be studied by electrical recording, but with considerable difficulty. The other population, the hilar mossy cell axons, are far too small for any existing electrical recording techniques.

Conclusions

hVOS probes can provide sufficiently strong signals and rapid response time to reveal action potential dynamics in neurons. This has been demonstrated by hVOS imaging of voltage from the cell somata of many classes of neurons, and in two classes of axons. Action potentials in somata produce rapid fluorescence changes that are readily detected, often in single trials. Action potential wave forms could be followed with high temporal fidelity to verify spike characteristics known to be specific to a particular type of neuron. Furthermore, action potential properties were shown to change dynamically in response to repetitive firing. These experiments have demonstrated the practical utility of studying action potential dynamics using hVOS probes, providing new insight into the intrinsic excitability in genetically-targeted cell types and revealing basic mechanisms of neural circuit computation.

Acknowledgements

Funded by NIH grants NS093866 and NS105200.

References

1. Connors BW, Gutnick MJ: Intrinsic firing patterns of diverse neocortical neurons. Trends Neurosci (1990) 13(3):99–104. [PubMed: 1691879]
2. Llinas RR: Intrinsic electrical properties of mammalian neurons and cns function: A historical perspective. Front Cell Neurosci (2014) 8(320.
3. Bean BP: The action potential in mammalian central neurons. Nature Rev Neurosci (2007) 8:451–465. [PubMed: 17514198]
4. Pedroni A, Minh do D, Mallamaci A, Cherubini E: Electrophysiological characterization of granule cells in the dentate gyrus immediately after birth. Front Cell Neurosci (2014) 8(44.
5. Scharfman HE, Myers CE: Hilar mossy cells of the dentate gyrus: A historical perspective. Front Neural Circuits (2013) 6(106.
6. Augustine GJ: Regulation of transmitter release at the squid giant synapse by presynaptic delayed rectifier potassium current. J Physiol (1990) 431(1):343–364. [PubMed: 1983120]
7. Sabatini BL, Regehr WG: Control of neurotransmitter release by presynaptic waveform at the granule cell to purkinje cell synapse. J Neurosci (1997) 17(10):3425–3435. [PubMed: 9133368]

8. Borst JG, Sakmann B: Effect of changes in action potential shape on calcium currents and transmitter release in a calyx-type synapse of the rat auditory brainstem. Philos Trans R Soc Lond B Biol Sci (1999) 354(1381):347–355. [PubMed: 10212483]

9. Aldrich RW, Getting PA, Thompson SH: Mechanism of frequency-dependent broadening of molluscan neurone soma spikes. Journal Physiol (1979) 291(1):531–544. [PubMed: 480247]

10. Gainer H, Wolfe J, Seth A, Lia Obaid AL, Salzberg BM: Action potentials and frequency-dependent secretion in the mouse neurohypophysis. Neuroendocrinology (1986) 43:557–563. [PubMed: 3018612]

11. Jackson MB, Konnerth A, Augustine GJ: Action potential broadening and frequency-dependent facilitation of calcium signals in pituitary nerve terminals. Proc Natl Acad Sci (1991) 88:380–384. [PubMed: 1988937]

12. Geiger JR, Jonas P: Dynamic control of presynaptic ca(2+) inflow by fast-inactivating k(+)channels in hippocampal mossy fiber boutons. Neuron (2000) 28:927–939. [PubMed: 11163277]

13. Casale AE, Foust AJ, Bal T, McCormick DA: Cortical interneuron subtypes vary in their axonal action potential properties. J Neurosci (2015) 35(47):15555–15567. [PubMed: 26609152]

14. Popovic M, Vogt K, Holthoff K, Konnerth A, Salzberg BM, Grinvald A, Antic SD, Canepari M, Zecevic D: Imaging submillisecond membrane potential changes from individual regions of single axons, dendrites and spines. Adv Exp Med Biol (2015) 859:57–101. [PubMed: 26238049]

15. Cho IH, Panzera LC, Chin M, Hoppa MB: Sodium channel beta2 subunits prevent action potential propagation failures at axonal branch points. J Neurosci (2017) 37(39):9519–9533. [PubMed: 28871036]

16. Loew LM, Cohen LB, Salzberg BM, Obaid AL, Bezanilla F: Charge-shift probes of membrane potential. Characterization of aminostyrylpyridinium dyes on the squid giant axon. Biophys J (1985) 47(1):71–77. [PubMed: 3978192]

17. Cohen LB, Salzberg BM, Davila HV, Ross WN, Landowne D, Waggoner AS, Wang CH: Changes in axon fluorescence during activity: Molecular probes of membrane potential. J Membr Biol (1974) 19(1):1–36. [PubMed: 4431037]

18. Ross WN, Salzberg BM, Cohen LB, Grinvald A, Davila HV, Waggoner AS, Wang CH: Changes in absorption, fluorescence, dichroism, and birefringence in stained giant axons:: Optical measurement of membrane potential. J Membr Biol (1977) 33(1–2):141–183. [PubMed: 864685]

19. Zecevic D: Multiple spike-initiation zones in single neurons revealed by voltage-sensitive dyes. Nature (1996) 381(6580):322–325. [PubMed: 8692270]

20. Popovic MA, Gao X, Carnevale NT, Zecevic D: Cortical dendritic spine heads are not electrically isolated by the spine neck from membrane potential signals in parent dendrites. Cereb Cortex (2014) 24(2):385–395. [PubMed: 23054810]

21. Rowan MJM, Tranquil E, Christie JM: Distinct kv channel subtypes contribute to differences in spike signaling properties in the axon initial segment and presynaptic boutons of cerebellar interneurons. J Neurosci (2014) 34:6611–6623. [PubMed: 24806686]

22. Ross WN, Miyazaki K, Popovic MA, Zecevic D: Imaging with organic indicators and high-speed charge-coupled device cameras in neurons: Some applications where these classic techniques have advantages. Neurophotonics (2015) 2(2):021005. [PubMed: 26157996]

23. Lou S, Adam Y, Weinstein EN, Williams E, Williams K, Parot V, Kavokine N, Liberles S, Madisen L, Zeng H, Cohen AE: Genetically targeted all-optical electrophysiology with a transgenic cre-dependent optopatch mouse. J Neurosci (2016) 36(43):11059–11073. [PubMed: 27798186]

24. Bayguinov PO, Ma Y, Gao Y, Zhao X, Jackson MB: Imaging voltage in genetically defined neuronal subpopulations with a cre recombinase-targeted hybrid voltage sensor. J Neurosci (2017) 37(38):9305–9319. [PubMed: 28842412] • Illustrates the potential of hVOS imaging with the full power of Cre-lox targeting technology.

25. Liu P, Grenier V, Hong W, Muller VR, Miller EW: Fluorogenic targeting of voltage-sensitive dyes to neurons. J Am Chem Soc (2017) 139(48):17334–17340. [PubMed: 29154543]

26. Grenier V, Daws BR, Liu P, Miller EW: Spying on neuronal membrane potential with genetically targetable voltage indicators. J Am Chem Soc (2019) 141(3):1349–1358. [PubMed: 30628785] • The detection of action potentials in subcellular compartments in a single trial.

27. Huang ZJ, Zeng H: Genetic approaches to neural circuits in the mouse. Annu Rev Neurosci (2013) 36:183–215. [PubMed: 23682658]
28. Storace D, Sepehri Rad M, Kang B, Cohen LB, Hughes T, Baker BJ: Toward better genetically encoded sensors of membrane potential. Trends Neurosci (2016) 39(5):277–289. [PubMed: 27130905]
29. Panzera LC, Hoppa MB: Genetically encoded voltage indicators are illuminating subcellular physiology of the axon. Front Cell Neurosci (2019) 13:52. [PubMed: 30881287] • A critical discussion of genetically-encoded voltage sensors and their applicability to action potential recording.
30. Hochbaum DR, Zhao Y, Farhi SL, Klapoetke N, Werley CA, Kapoor V, Zou P, Kralj JM, Maclaurin D, Smedemark-Margulies N, Saulnier JL et al.: All-optical electrophysiology in mammalian neurons using engineered microbial rhodopsins. Nat Methods (2014) 11(8):825–833. [PubMed: 24952910]
31. Kannan M, Vasan G, Pieribone VA: Optimizing strategies for developing genetically encoded voltage indicators. Front Cell Neurosci (2019) 13(53.
32. Hoppa MB, Gouzer G, Armbruster M, Ryan TA: Control and plasticity of the presynaptic action potential waveform at small cns nerve terminals. Neuron (2014) 84:778–789. [PubMed: 25447742]
33. Ford KJ, Davis GW: Archaerhodopsin voltage imaging: Synaptic calcium and bk channels stabilize action potential repolarization at the drosophila neuromuscular junction. J Neurosci (2014) 34(44):14517–14525. [PubMed: 25355206]
34. Chanda B, Blunck R, Faria LC, Schweizer FE, Mody I, Bezanilla F: A hybrid approach to measuring electrical activity in genetically specified neurons. Nat Neurosci (2005) 8(11):1619–1626. [PubMed: 16205716] • The invention of hVOS imaging.
35. Hodgkin AL, Huxley AF: A quantitative description of membrane current and its application to conduction and excitation in nerve. J Physiol (1952) 117(4):500–544. [PubMed: 12991237]
36. Wang D, Zhang Z, Chanda B, Jackson MB: Improved probes for hybrid voltage sensor imaging. Biophys J (2010) 99:2355–2365. [PubMed: 20923671]
37. Lu CC, Kabakov A, Markin VS, Mager S, Frazier GA, Hilgemann DW: Membrane transport mechanisms probed by capacitance measurements with megahertz voltage clamp. Proc Natl Acad Sci (1995) 92(24):11220–11224. [PubMed: 7479969]
38. Fernández JM, Taylor RE, Bezanilla F: Induced capacitance in the squid giant axon. Lipophilic ion displacement currents. J Gen Physiol (1983) 82(3):331–346. [PubMed: 6631402]
39. Benz R, Nonner W: Structure of the axolemma of frog myelinated nerve: Relaxation experiments with a lipophilic probe ion. J Membr Biol (1981) 59(2):127–134. [PubMed: 6264083]
40. Bradley J, Luo R, Otis TS, DiGregorio DA: Submillisecond optical reporting of membrane potential in situ using a neuronal tracer dye. J Neurosci (2009) 29(29):9197–9209. [PubMed: 19625510]
41. Ghitani N, Bayguinov PO, Ma Y, Jackson MB: Single-trial imaging of spikes and synaptic potentials in single neurons in brain slices with genetically encoded hybrid voltage sensor. J Neurophysiol (2015) 113: 1249–1259. [PubMed: 25411462]
42. Feng G, Mellor RH, Bernstein M, Keller-Peck C, Nguyen QT, Wallace M, Nerbonne JM, Lichtman JW, Sanes JR: Imaging neuronal subsets in transgenic mice expressing multiple spectral variants of gfp. Neuron (2000) 28(1):41–51. [PubMed: 11086982]
43. Ma Y, Bayguinov PO, Jackson MB: Action potential dynamics in fine axons probed with an axonally targeted optical voltage sensor. eNeuro (2017) 4:(4).• The first use of a genetically-encoded voltage sensor targeted to a cellular compartment.
44. Debanne D, Campanac E, Bialowas A, Carlier E, Alcaraz G: Axon physiology. Physiol Rev (2011) 91(2):555–602. [PubMed: 21527732]
45. Wang D, McMahon S, Zhang Z, Jackson MB: Hybrid voltage sensor imaging of electrical activity from neurons in hippocampal slices from transgenic mice. J Neurophysiol (2012) 3147–3160. [PubMed: 22993267]

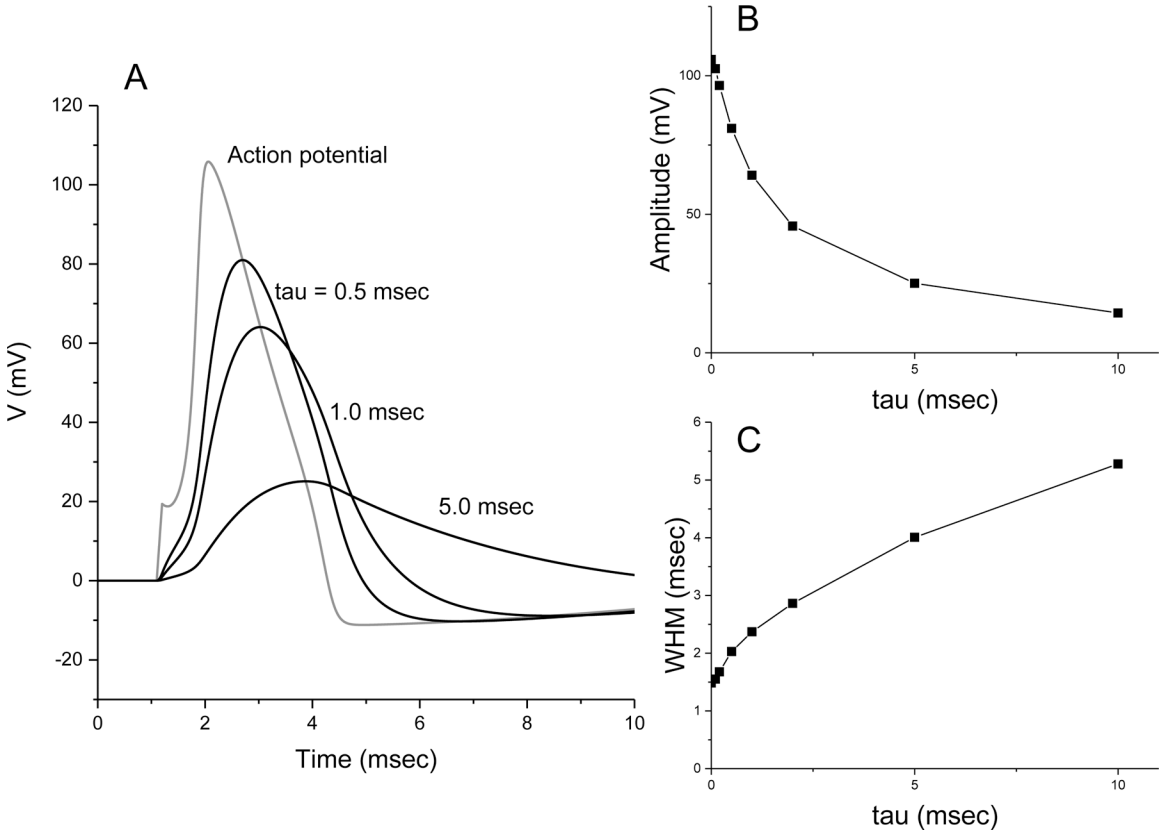

Figure 1.

Mathematical analysis of action potential filtering by detectors with different response times. **A**. Plots of voltage versus time for an action potential simulated by integrating the Hodgkin-Huxley equations (gray trace), and by filtering this waveform according to Eq. 3 with the indicated sensor time constants (tau; black traces). Note the uptick in the Hodgkin-Huxley spike at 1.1 msec reflects the brief 0.1 msec current pulse added mathematically to trigger the spike. **B.** Plot of amplitude versus tau. **C.** Plot of width at half maximum (WHM) versus tau.

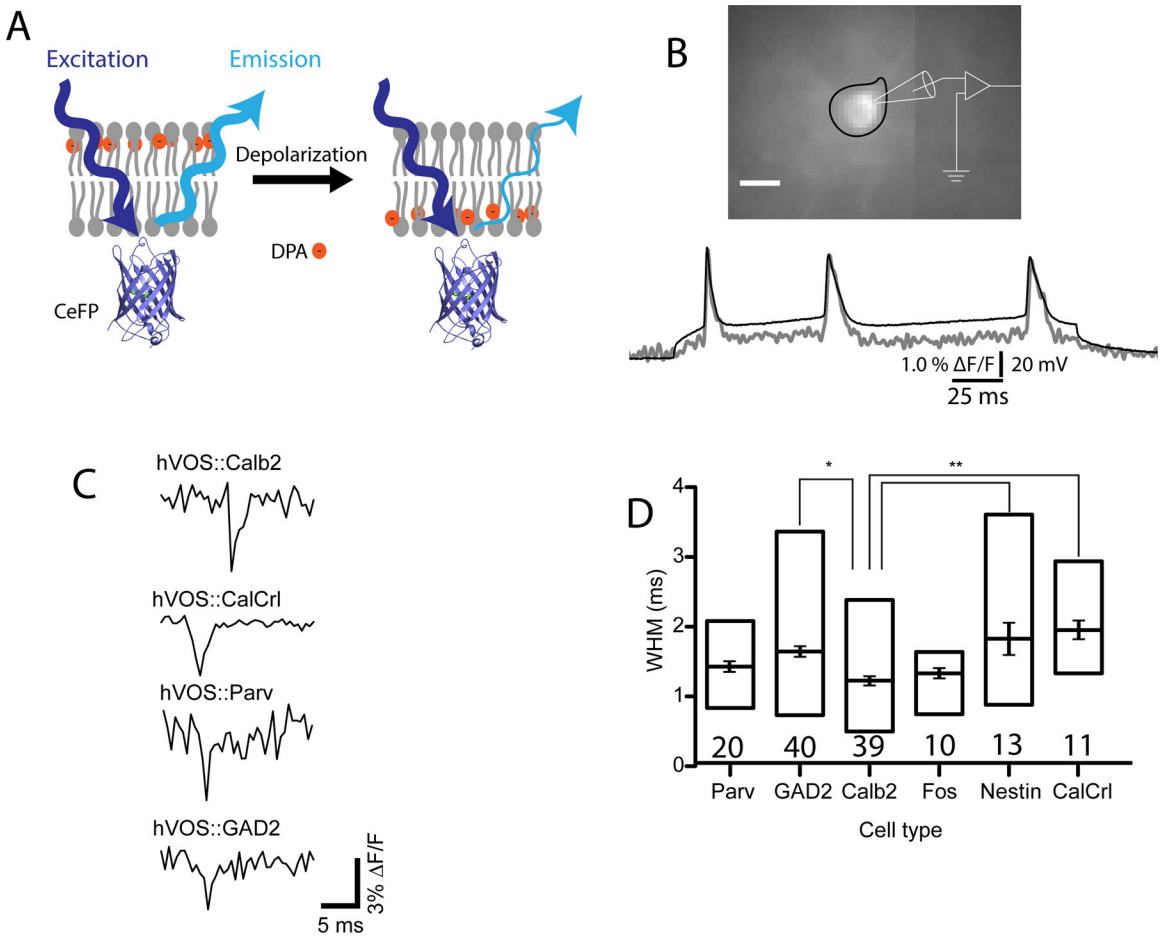

Figure 2.

hVOS imaging of action potentials. **A.** Illustration of the hVOS sensing mechanism. The probe is cerulean fluorescent protein (CeFP) tethered to the inner face of the plasma membrane by farnesylation of the truncated h-ras motif appended to the C-terminus [36]. The orange circles represent the negatively charged, lipophilic molecule dipicrylamine (DPA). Negative potentials at rest drive DPA to the extracellular face (left). Because DPA is far from the CeFP, fluorescence emission is strong. Depolarization drives DPA to the inner face (right). The shorter distance between the DPA and CeFP strengthens the FRET interaction to reduce fluorescence emission. **B.** A neuron expressing hVOS probe in the entorhinal cortex in a brain slice. The neuron is fluorescent and its cell body is outlined in black. A patch clamp recording under current clamp displays three action potentials evoked by a 200 msec current step (black trace). The fluorescence decreased during the spikes and the fluorescence trace (gray) was inverted to make the spike positive for easy comparison. The fluorescence follows the voltage trace with excellent temporal fidelity (panel B reproduced from [41]). **C.** hVOS probe was targeted to various cell types by crossing an hVOS Cre reporter mouse with various Cre drivers [24]. Extracellular stimulation elicited action potentials in four different types of neurons, a calretinin-expressing interneuron (calb2), a hilar mossy cell defined by expression of the calcitonin receptor like receptor (CalCrl), a parvalbumin-expressing interneuron (Parv), and a GABAergic interneuron

defined by expression of glutamic acid decarboxylase (GAD2). **D.** Width at half maximum (WHM) averaged for the indicated number of cells (mean, standard error, and range). Nestin labels adult-born granule cells in the dentate gyrus; Fos labels granule cells activated by experiencing a novel environment. The GAD2 and Calb2 values differed significantly ($p<0.05$). The Calb2 value was significantly different from both the Nestin and CalCrl values ($p<0.01$). (panels C and D reproduced from [24]).

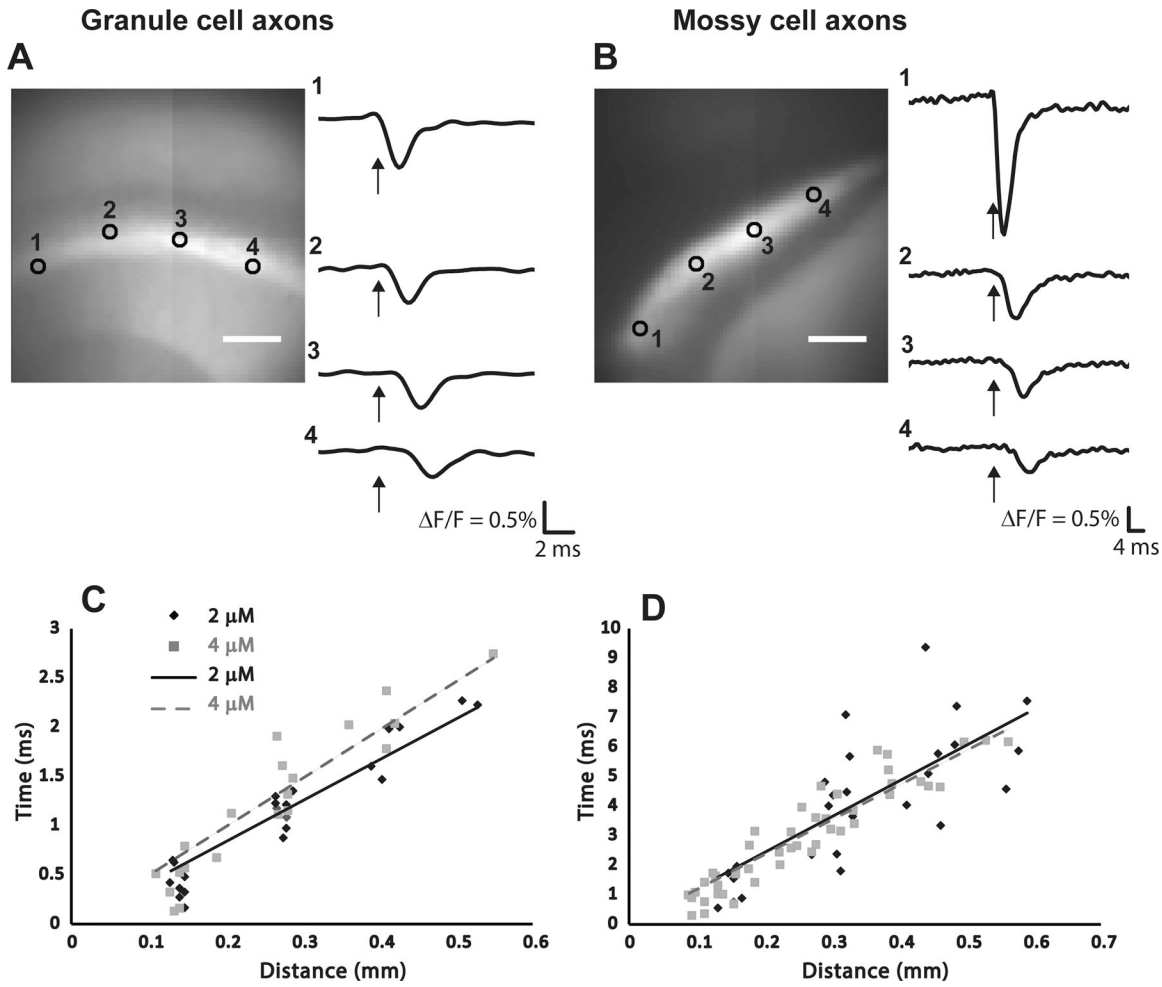

Figure 3.

Action potential propagation in the axons of granule cells and mossy cells. The hVOS probe illustrated in Fig. 2A was modified to incorporate a motif from GAP43 [36], which resulted in axon targeting [43,45]. In hippocampal slices prepared from a transgenic mouse with this probe on the thy1 promotor, probe expression was evident in the mossy fibers of the stratum lucidum in the CA3 region, formed by granule cell axons (**A**), and in a population of axons in the inner molecular layer of the dentate gyrus, formed by hilar mossy cells (**B**). Stimulation near the sites numbered *1* elicited a fluorescence change that propagated to the more distant sites over a few msec (recording sites numbered in the images to the left correspond to numbers of the traces to the right). Plots of time versus distance for granule cell axons (**C**) and mossy cell axons (**D**) illustrate propagation with constant velocity. Black diamond and solid line, 2 μM DPA; grey square and dashed gray line, 4 μM DPA. The legend in **C** also applies to **D**. Velocities determined from these plots are stated in the text (reproduced from [43]).

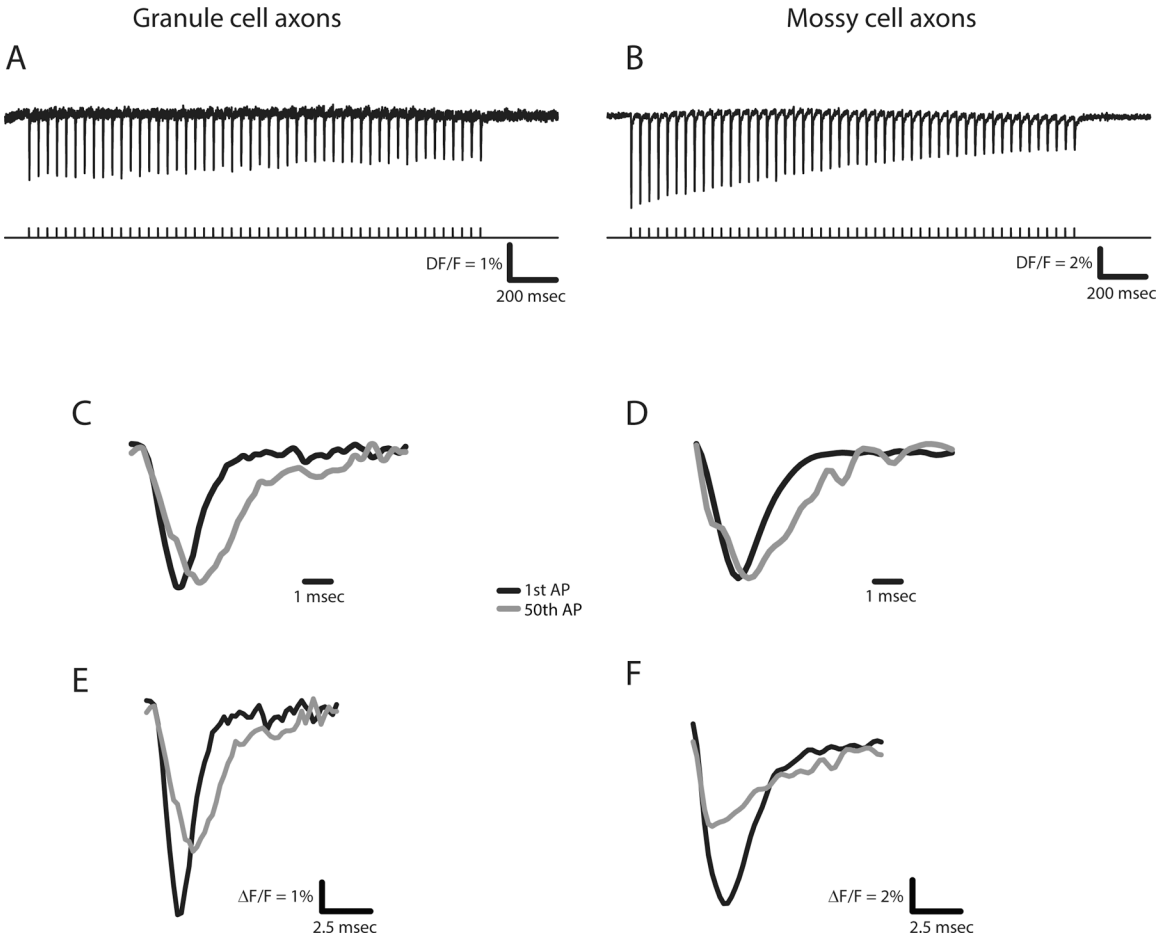

Figure 4.

Activity-dependent changes in action potentials determined with the axonally targeted hVOS probe described in Fig. 3. Action potentials elicited by a 25 Hz train of 50 pulses in the axons of granule cells (**A**) and mossy cells (**B**). The first and last action potentials seen in the hVOS signals from each train were superimposed (**C** and **D**). Normalization to the peak fluorescence change highlights the differences in breadth (WHM). First and last action potentials are superimposed without normalization to highlight the reduction in amplitude (**E** and **F**). (reproduced from [43], see this paper for quantitative analysis of action potential broadening and attenuation).